The following publication C. Li, X. Gao, S. Fan, D. Wang and W. Jin, "Measurement of the Adhesion Energy of Pressurized Graphene Diaphragm Using Optical Fiber Fabry–Perot Interference," in IEEE Sensors Journal, vol. 16, no. 10, pp. 3664-3669, May15, 2016 is available at https://doi.org/10.1109/JSEN.2016.2536783.

Measurement of the Adhesion Energy of Pressurized Graphene Diaphragm using Optical Fiber Fabry-Perot Interference

Li Cheng, Gao Xiangyang, Fan Shangchun, *Senior Member, IEEE*, Wang Dongxue, and Jin Wei, *Senior Member, IEEE*

***Abstract*—Van der Waals adhesion between graphene and substrate has an important impact on the graphene-based sensor performance. Here we proposed a simple in situ measurement method for adhesion energy of graphene diaphragm suspended on the endface of a ferrule. The interaction between the diaphragm and its substrate created a low finesse Fabry-Perot (FP) interferometer. The analytical relationship between prestress and adhesion energy was modeled on the basis of the initial dip along the edges of the suspended regions. Then, the deflection deformations of pressurized graphene diaphragm were examined using FP interference technology. The obtained adhesion energies for monolayer and two to five layer graphene membranes on SiO_2 conformed exceedingly well to the previously measured results and yielded a cross-correlation coefficient of 0.999 with the latter. Furthermore, an experimental setup for acoustic pressure test was developed to determine the adhesion energies for ~7-layer and ~13-layer graphene diaphragms with a zirconia substrate to be 0.286 J/m^2 and 0.275 J/m^2, respectively. The highly consistent experimental data confirmed the accuracy of our method. This method presented in this paper could be further extended for measuring the adhesion energy of other 2D materials.**

***Index Terms*—Graphene diaphragm, adhesion energy, pressure-deflection behavior, prestress, Fabry-Perot interference**

I. Introduction

GRAPHENE, with a single-layer thickness of ~0.335 nm, is being utilized more since it was first isolated by Novoselov *et al.* [1] because of its extreme elasticity [2], ultrastrong adhesion [3], impermeability to gases [4], optical far-infrared properties [5] and thermal sensitive characteristics [6]. The unique combination of electronic and mechanical properties makes graphene an ideal material for sensor applications involving electromechanical coupling, such as micro- and nano-electromechanical (MEMS/NEMS) sensors and actuators [7-9]. However, at the nano-scale, the surface forces are so very strong and flexible so as to make graphene membranes interact and adhere strongly to materials and structures in its vicinity. Therefore, measuring and grasping the nature of adhesion energy between graphene and various substrates is necessary for graphene-based nano-mechanical and nano-electric devices [10].

In recent years, a few theoretical and experimental studies of the adhesion of the graphene membrane-substrate interface have been reported [11-19]. He *et al.* developed a theoretical method to calibrate the interface adhesion energy of monolayer and multilayer graphene on substrates based on the bond relaxation model for the interfaces including graphene/SiO_2, graphene/Cu, graphene/Cu/Ni and Cu/graphene/Ni [12]. Zong *et al.* mechanically exfoliated graphene adhered to a SiO_x surface covered with ~50-80 nm diameter gold and silver nanoparticles, thereby achieving a graphene-SiO_x adhesion energy of 0.15 J/m^2 by taking Young's modulus E=0.5 TPa [13]. However, if E=1 TPa, the adhesion energy would be 0.3 J/m^2 [14]. After that, Koenig *et al.* directly measured the adhesion energy of 0.45 ± 0.02 J/m^2 for monolayer graphene and 0.31 ± 0.03 J/m^2 for samples containing two to five layer graphene sheets by using a pressurized blister test [15]. Further experiment by Boddeti *et al.* showed the average adhesion energy values of 0.44 J/m^2 and 0.24 J/m^2 for two different sets of monolayer graphene blisters fabricated on two different chips by atomic force microscope (AFM) indentation experiments [16]. In addition, Yoon *et al.* found that the adhesion energy of large-area monolayer graphene on copper was 0.72 ± 0.07 J/m^2 by double cantilever beam fracture mechanics testing [17]. Then Das *et al.* reported that the adhesion energies of chemically vapor deposited (CVD) graphene on Cu and Ni substrates were measured to be 12.8 and 72.7 J/m^2, respectively [18]. Recently, Jiang *et al.* converted the adhesion forces measured by AFM with a microsphere tip to the adhesion energies of monolayer graphene on SiO_2 and Cu, which were 0.46 and 0.75 J/m^2, respectively [19].

This work was supported by the National Nature Science Fund of China (61573033), the Program for Changjiang Scholars and Innovative Research Team in University (IRT1203), the Aviation Science Foundation of China (20152251018) and the Graduate Innovation Fund of Beihang University (YCSJ-01-2015-01).

Li Cheng is with the School of Instrumentation Science and Opto-electronics Engineering, Beihang University, Beijing 100191 China (*Corresponding author*, email: licheng@buaa.edu.cn).

Gao Xiangyang is with the School of Instrumentation Science and Opto-electronics Engineering, Beihang University, Beijing 100191 China (email: xiangyang1023@163.com).

Fan Shangchun is with the School of Instrumentation Science and Opto-electronics Engineering, Beihang University, Beijing 100191 China (email: fsc@buaa.edu.cn)

Wang Dongxue is with Jinan University, Jinan 250022 China (email: wdongxue18@163.com).

Jin Wei is with the Department of Electrical Engineering, The Hong Kong Polytechnic University, Hong Kong, China (email: eewjin@polyu.edu.hk)

Accordingly, these experimental studies have significantly advanced the understanding of graphene adhesion behaviors. However, these approaches to determine the adhesion energy of graphene and a substrate typically involve experiments where graphene in adhesive contact with a substrate is delaminated from it by well-controlled forces [14]. Moreover, specific measurement setups and complicated sample test process are generally needed. Here from the viewpoint of graphene-based device performance instead of graphene sample analysis, we reported a simple in situ nano-scale quantification study of the adhesion energy of CVD graphene on certain substrates such as SiO_2 and zirconia (ZrO_2). A multilayer graphene sheet cut from a commercial sample were transferred onto the endface of a zirconia ferrule to form a FP sensor in order to measure the deformation of graphene conforming to well-defined surface features, which contributed to evaluating the effect of the interface adhesion on graphene-based micro/nano devices. Along with the pressure-deflection relationship integrating the balance between adhesion energy and strain energy at equilibrium, the calculated adhesion energies for 1-5 layers and multilayer of graphene, respectively, on SiO_2 and ZrO_2 were exceedingly well agreement with the previous theoretical and experimental results.

II. Model Adapted to the Method

A. Principle of the FP Sensor with Graphene Diaphragm

Figure 1(a) shows the schematic diagram and the physical picture of the presented FP sensor that comprises of a zirconia ferrule with a bore diameter of 125 μm, a standard single mode fiber (SMF) and a suspended multilayer graphene diaphragm. The diaphragm, working as a light reflector made directly on the end of the SMF, was adhered to the zirconia substrate by van der Waals forces as shown in Fig. 1(b), and the separation between the fiber end and the ferrule endface was controlled by using a 1-μm resolution translation stage. The ferrule and the SMF were held together by an epoxy adhesive (3M®). The graphene diaphragm was prepared from a commercial Trivial Transfer Graphene (TTG) sample in which the graphene membrane was grown by chemical vapor deposition (CVD) on a 20-μm thick Cu foil deposited on a polymer substrate (ACS Material®, www.xfnano.com). The process for preparing the graphene membrane and transferring it onto the fiber tip to an FP cavity is similar to that in Ref.[20].

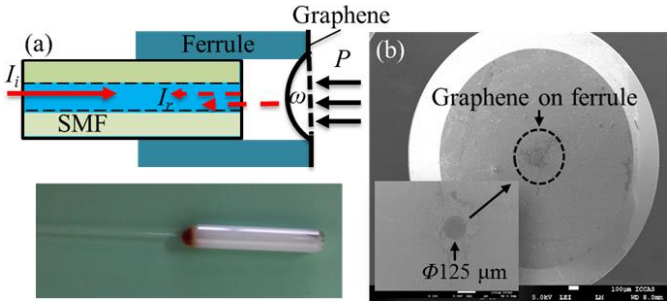

Fig. 1. (a) Schematic diagram and physical picture of the FP sensor and (b) microscopic image of graphene diaphragm adhered on the ferrule endface.

As seen in Fig.1(a), when an external pressure was applied to the diaphragm, its deformation caused the length of FP cavity to change. For the purpose of modeling the load-deflection behavior, the sensor was approximated as a clamped circular diaphragm made of a linear isotropic elastic material based on the spherical shell equation. The relationship between the diaphragm deflection ω and the pressure difference P may be expressed as [21]

$$P=\frac{4\sigma_0 t}{r^2}\omega+\frac{8Et\omega^3}{3(1-\upsilon)r^4}, \tag{1}$$

where E is the Young's modulus of graphene (~1 TPa); r, t, υ and σ_0 are the radius, the thickness, the Poisson's ratio (~0.17) and the prestress of graphene diaphragm, respectively.

Due to the FP interference [22], the interference intensity I_r in the FP cavity for diaphragm-type optical fiber sensors can be approximated as

$$I_r=\left(R_2+\xi R_1-2\sqrt{\xi R_1 R_2}\cos\delta\right)I_i, \tag{2}$$

where R_1 and R_2 (typically 0.025) are the reflective values of the graphene diaphragm and the fiber end/air interface, respectively; I_i is the incident intensity from the laser; ξ is the coupling coefficient of cavity length loss, which can be calculated as mentioned in the reference [23]; δ is the phase difference between two adjacent beams in micro-air cavity, which can be approximated as $4\pi L/\lambda$, where L is the length of FP cavity and λ is the wavelength of incident light.

In this case, the interference intensity (ΔI) caused by the FP cavity length change (ΔL) due to applied external load P may be described as

$$\Delta I=\frac{8\pi}{\lambda}I_i\sin\frac{4\pi L}{\lambda}\sqrt{\xi R_1 R_2}\Delta L. \tag{3}$$

In fact, the wavelength of a tunable laser can be tuned to the quadrature point of an interference fringe to maximize the acoustic sensitivity for the interference intensity demodulation [24]. That is, δ may be adjusted to be $k\pi+\pi/2$, where k is a nature number. As a result, the measured deflection ω of the diaphragm is resolved to be [25]

$$\omega=\frac{\lambda\left(R_2+\xi R_1\right)\Delta I}{8\pi I_i\sqrt{\xi R_1 R_2}}. \tag{4}$$

Hence the pressure-deflection behavior of the FP sensor with graphene diaphragm can be measured by the output voltage from a photo-detector (PD).

B. Pressure-Deflection Deformation under Prestress

According to (4), there is no change in the deflection of graphene diaphragm when no external loads are applied. However, Bunch *et al.* fabricated and measured the first graphene drum resonators, which showed self-tensioning in the graphene resonators due to adhesion to the sidewalls by the van der Waals forces that clamped the graphene membrane to a substrate [10]. The magnitude of the tension (0.1 N/m) was deduced from the resonant frequency and verified by AFM indentation experiments when the pressure change P=0 at both sides of graphene membrane [15]. The adhesion to the sidewalls was also seen by Lee *et al.*, but the magnitude was an order of magnitude smaller than that measured by Bunch *et al.* [14]. Moreover, dips of several nanometers along the edges of

the suspended regions, where the graphene membrane met the SiO_2 sidewalls, were also obtained by AFM indentation experiments by both groups. In this case, the interplay between the initial tension-dependent graphene-substrate adhesion energy and the graphene deformation plays a key role in determining the equilibrium graphene conformation [26].

Referring to Fig.2, the edge of suspended circular graphene membrane is adhered onto the sidewalls of the ferrule because of the strong van der Waals interaction. We presented a mechanics analytical model that describes the balance between adhesion energy and strain energy at equilibrium, where the graphene membrane is flat due to the adhesion behavior and the pressures inside and outside the FP cavity are equal initially. Hence the equilibrium configurations of the deformed membrane can be determined by seeking minima in the total free energy U which can be expressed as [12]

$$U = U_{mem} + U_{adh}, \tag{5}$$

where U_{adh} is the adhesion energy of the membrane-substrate interface, and U_{mem} is the elastic strain energy stored in the membrane as it deforms when subjected to stretching and bending. It is noted that the bending energy for the flexible graphene sheets is neglected in (5) because self-tensioning in these thin sheets dominates over the bending rigidity.

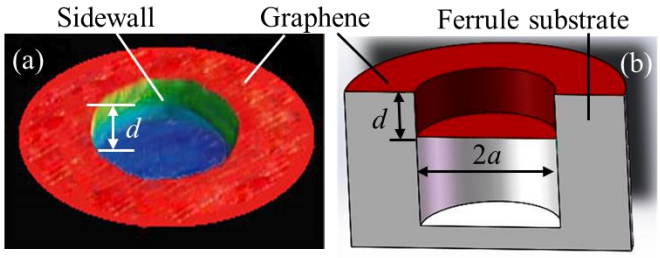

Fig. 2. (a) Schematic of the graphene membrane with an initial deflection d and (b) structure model of the graphene membrane adhered to the ferrule endface.

For a constant value of adhesion energy per unit area Γ, U_{adh}, an external force potential energy, is then

$$U_{adh} = -2\pi a d\Gamma. \tag{6}$$

Only considering stretching, U_{mem} is simplified as

$$U_{mem} = \frac{1}{2}\iint_A \left(N_r\varepsilon_r + N_t\varepsilon_t\right) r\mathrm{d}r\mathrm{d}\theta, \tag{7}$$

where N_r and ε_r are respectively the tension and the strain in the radial direction of membrane; N_t and ε_t are respectively the tension and the strain in the circumferential direction of membrane; and A is the area of the interface between the membrane and the substrate sidewall. By solving the radial displacement in an annular membrane [27], U_{mem} is rewritten as

$$U_{mem} = \iint_A \frac{Et}{1-\nu}\left(\frac{d}{a}\right)^2 r\mathrm{d}r\mathrm{d}\theta = \pi a t\sigma_0 d. \tag{8}$$

By seeking minima in the total free energy U from (6) and (8), the relationship between Γ and σ_0 at initial equilibrium yields

$$\Gamma = \frac{t\sigma_0}{2}. \tag{9}$$

Equation (9) shows that the adhesion energy between graphene membrane and the substrate is associated with the initial prestress and the film thickness. By substituting (9) into (1), Γ can be calculated by

$$\Gamma = \frac{Pa^2}{8\omega} + \frac{Et\omega^3}{3(1-\upsilon)a^2}. \tag{10}$$

III. Experiment and Analysis

It can be inferred from (10) that the pressure-deflection characteristics of graphene diaphragm can be improved by exploring adhesion behaviors of the membrane-substrate interface. In other words, Γ can be confirmed by the pressure-deflection characteristics of diaphragm. Based on the actual static pressure-deflection data measured by AFM experiments in Ref.[10], we solved the corresponding adhesion energies as illustrated in Fig.3, in terms of (10) mentioned above instead of complicated constant N blister companion experiments used in the reference.

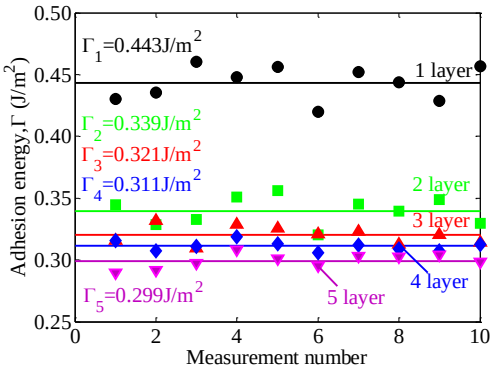

Fig. 3. Calculated adhesion energy for graphene membrane on SiO_2.

The average calculated results were labeled by the symbol '△' (regular triangle) in Fig.4, where the adhesion energy for monolayer graphene was set as 0.443 J/m^2, in excellent agreement with 0.46 J/m^2 in Ref.[19]. Moreover, the calculated adhesion energies for 1 to 5-layer graphene on SiO_2 were well consistent with those of Refs.[12, 15], and yielded a cross-correlation coefficient of 99.88% and 99.96%, respectively, with them marked by the symbols '○' (circle) and '◊' (diamond). The slight deviation between the data in this paper and the Ref.[12] is possibly due to the presence of the impurities on graphene membrane and substrate surface topography. It is noticed that the difference gradually becomes smaller as the number of layers increases, which also proves the decreasing effect of substrate surface topography because of reduced roughness with increasing layer number.

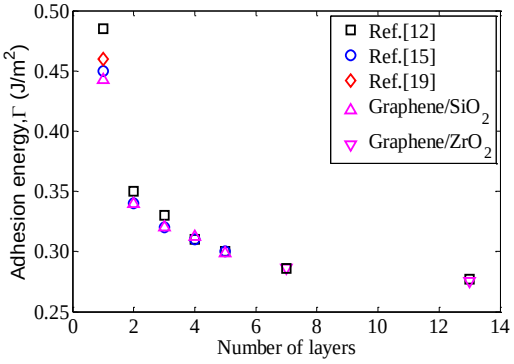

Fig. 4. Dependence of adhesion energy on the membrane thickness.

To further verify the proposed model, an experimental setup for acoustic pressure test in Fig.5(a) was developed to quantify dynamic (acoustic) pressure-deflection responses of FP sensor for measuring the adhesion energy of graphene diaphragm with a ferrule substrate. A reference microphone (MP201) with a sensitivity of 50.7 mV/Pa and a developed FP sensor were placed inside of an acoustic isolation chamber in Fig.5(b), where the distance between the loudspeaker and the two sensors was about 1 m. Two commercial TTG samples (6~8 layer and 10~15 layer) were employed to fabricate two FP sensors with different membrane thicknesses. A tunable laser illuminated the FP sensor at a wavelength of 1550 nm, and the interference intensity was detected by a PD with a preamplifier through the use of an optical circulator. The MP201 provided a reference acoustic pressure for the FP sensor. In advance of the acoustic pressure test, the acoustic signal generated by the loudspeaker was initially calibrated to achieve a standard acoustic pressure of 1 Pa at 1 kHz with the aid of the reference microphone and software compensation method.

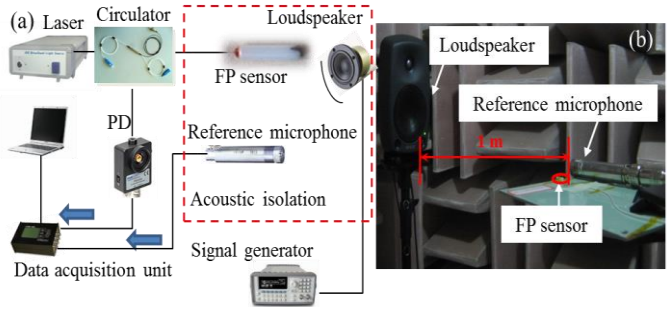

Fig. 5. (a) Experimental setup for acoustic pressure test and (b) picture of device arrangement in an anechoic chamber.

However, it is vital to firstly determine the reflectivity R_1 of the graphene diaphragm suspended onto the fiber-tip from (4). It should be pointed out that the reflectance and transmittance of graphene in the optical region are also a function of wavelength of incident light and membrane thickness. In accordance with the wavelength range (1528-1608 nm) of used broadband source (ALS-CL-17), R_1 can be calculated by the complex refractive index [20, 28, 29] and fitted by the measured interference spectrums of the FP sensor via an optical spectrum analyzer (AQ6370C). In this case, the reflectivities of the two 6~8-layer and 10~15-layer graphene membranes were averaged to be 0.652% and 1.49%, respectively, based on a 3σ rule, in close proximity to the calculated those of 0.727% and 1.72% for ~8-layer and ~13-layer membranes. Hence by taking the FP sensor with the ~13-layer graphene diaphragm as an example, its frequency response to sensitivity was investigated [30], which was relatively flat with a fluctuation of less than 7.5 dB in the range of 1 kHz to 20 kHz as shown in Fig.6. The sensitivity at 1 kHz approached -20 dB. Unfortunately, the sensor tended to exhibit an inferior response performance at frequencies lower than 100 Hz. The phenomenon was mainly due to the leakage of sealed air in the FP cavity, thereby resulting in a preferable acoustic pressure response at higher frequencies. In generally, due to the advantage of extremely thin thickness, graphene diaphragm is available to offer higher pressure sensitivity in comparison with those made with other materials. Also, the high Young's modulus (~1 TPa) allows graphene diaphragm to have a higher fundamental frequency. Then the deflection deformation of graphene diaphragm was examined by (10) when subjected to dynamic acoustic pressures at a better frequency of 16 kHz in Fig.6. The applied acoustic pressures, calibrated by the MP201's output electrical signals and the sensitivity of 50.7 mV/Pa, were recorded.

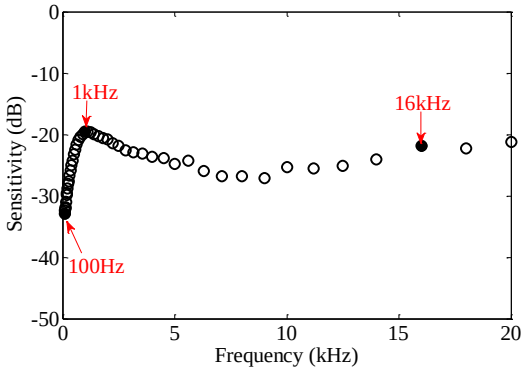

Fig. 6. Frequency response of the FP sensor at 1/3 octave band frequencies.

It is important to note that acoustic pressure excitations at other frequencies are also available for the determination of adhesion energy, which has no effect on the final result of Γ. Figure 7 shows the actual diaphragm deflections induced by these acoustic pressures. The measured data were fitted with a sensitivity of 2.22 nm/Pa by an over-sampling and linear least-squares method with a fitting coefficient of 99.7%. From Eq.(10), each pair of acoustic pressure-deflection points can determine an adhesion energy value, thus producing multiple Γ values due to several pairs of points as shown in Fig.8 similar to Fig.3. Then Γ for ~13-layer graphene membrane on ZrO_2 was averaged to be 0.275 J/m^2, which was described well with the theoretical value of 0.277 J/m^2 on SiO_2 in Ref.[12] shown in Fig.4. The lower measured value is due to the crystalline structure of ZrO_2 at normal temperature, in contrast to the amorphous structure of SiO_2 which allows graphene to conform well to the substrate [31]. Consequently, the corresponding prestress was set as 0.1 GPa. By taking this prestress value into (1) again, a theoretical linear sensitivity of 2.25 nm/Pa was achieved, which was very close to the measured sensitivity shown by solid circle in Fig.7. Additionally, from the Hencky's series solutions by Campbell J.D. [32], the condition for linear deflection deformation of (1) can be derived by

$$\frac{4(1-\upsilon)\sigma_0}{E}\left(\frac{Et}{Pa}\right)^{2/3} >> 1. \tag{11}$$

In this way,

$$P << \frac{16}{a}\left[\frac{2(1-\upsilon)^3\Gamma^3}{Et}\right]^{1/2} = P_c. \tag{12}$$

From (12), P_c was theoretically set as about 60 Pa for the developed FP sensor with ~13-layer graphene diaphragm. In the same way, for the FP sensor with ~7-layer graphene diaphragm, a group of acoustic pressure-deflection responses at 11 kHz was extracted to approximate Γ for ~7-layer graphene

as 0.286 J/m^2 (Fig.8) , in close to the theoretical value of 0.287 J/m^2 on SiO_2 in Ref.[12], with a corresponding prestress of 0.2 GPa. Thus a theoretical linear sensitivity of 1.69 nm/Pa was achieved, which also agreed with the measured sensitivity of 1.66 nm/Pa shown by solid square in Fig.7. Compared with previously reported diaphragm-based fiber-tip FP pressure sensors using different types of elastic materials as a pressure-sensitive diaphragm such as chitosan, polymer, SiO_2/silica and silver membrane [33-36], the sensor presented here used a thinner diaphragm and exhibited a much higher dynamic (acoustic) pressure sensitivity. In addition, P_c was then theoretically calculated as around 90 Pa. The experimental results showed that the linear operation confine of diaphragm-type FP sensor available was obviously limited by adhesion energy and membrane thickness. Owing to reduced Γ with increasing layer number, the range of P_c would be monotonously narrowed accordingly. In view of the membrane-substrate adhesion mechanism, further research on the performance optimization in FP sensors using graphene diaphragm is needed to investigate the physics behind it.

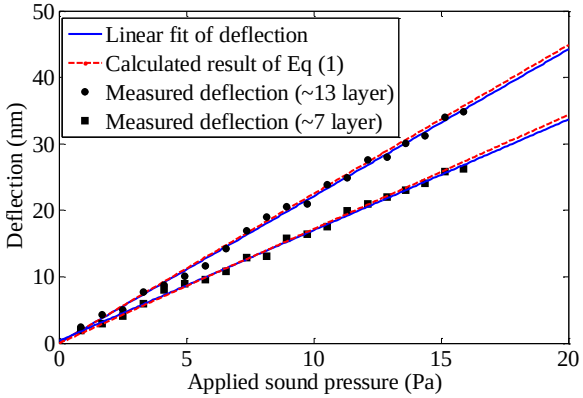

Fig. 7. The measured and theoretical acoustic pressure-deflection responses of FP sensors with ~7-layer and ~13-layer graphene diaphragms.

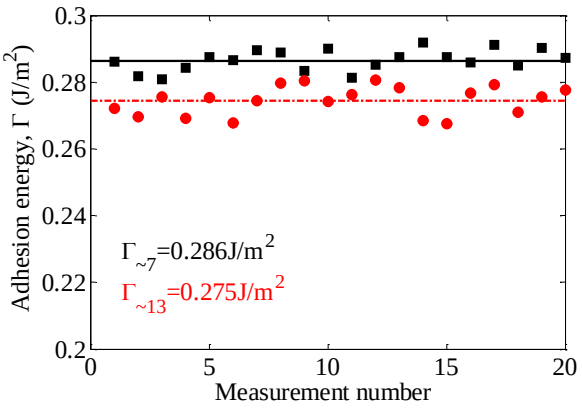

Fig. 8. Measured adhesion energy for graphene membrane on ZrO_2.

IV. Conclusion

A simple in situ method using the FP interference was demonstrated to detect the pressure-deflection behaviors of graphene diaphragm, working as a light mirror of a FP interferometer, so as to measure the adhesion energy between a few layers of graphene and the different substrates (SiO_2, ZrO_2). With the pressure-deflection responses measured by Koennig *et al.* using a pressurized blister test, we successfully deduced the adhesion energies on SiO_2 by incorporating the model of relationship between prestress and adhesion energy with regard to the initial dip along the edges of the suspended regions, which conformed well to the previously obtained theoretical and experiment results. Afterwards, the dynamic acoustic pressure-deflection responses of ~7-layer and ~13-layer graphene diaphragms adhered to the endface of a ZrO_2 ferrule, respectively, were examined to solve the adhesion energies of 0.286 and 0.275 J/m^2 accordingly, in exceeding agreement with the adhesion energy theoretical solutions of graphene with the same layer thickness on SiO_2. For this reason, this developed approach will open a new direction to evaluate the adhesion characteristics between a wide range of 2D-nanomaterial and various substrates.

References

[1] K.S. Novoselov, A.K. Geim, S.V. Morozov, D. Jiang, Y. Zhang, S.V. Dubonos, I.V. Grigorieva and A.A. Firsov, "Electric field effect in atomically thin carbon films", *Science*, vol. 306, no. 5696, pp. 666-669, Oct. 2004.

[2] C. Lee, X. Wei, J.W. Kysar and J. Hone, "Measurement of the elastic properties and intrinsic strength of monolayer graphene", *Science*, vol. 321, no. 5887, pp. 385-388, July. 2008.

[3] Z. Lu and M.L. Dunn, "van der Waals adhesion of graphene membranes", *J. Appl. Phys.*, vol. 107, pp. 044301, Feb. 2010.

[4] J.S. Bunch, S.S. Verbridge, J.S. Alden, A.M. van der Zande, J.M. Parpia, H.G. Craighead and P.L. McEuen, "Impermeable atomic membranes from graphene sheets", *Nano Letters*, vol. 8, no. 8, pp. 2458-2462, June. 2008.

[5] F. Bonaccorso, Z. Sun, T. Hasan and A.C. Ferrari, "Graphene photonics and optoelectronics", *Nature Photonics*, vol. 4, pp. 611-622, Aug. 2010.

[6] B.Y. Cao, W.J. Yao and Z.Q. Ye, "Networked nanoconstrictions: An effective route to tuning the thermal transport properties of graphene", *Carbon*, vol. 96, pp. 711-719, Sep. 2016.

[7] A. Rinaldi, A. Proietti, A. Tamburrano, M. Ciminello and M.S. Sarto, "Graphene-based strain sensor array on carbon fiber composite laminate", *IEEE Sensors Journal*, vol. 15, no. 12, pp. 7295-7303, Dec. 2015.

[8] D.S. Anderson, V. Sam, N. Frank, C.F. Andreas, S. Mikael, D. Anna, O. Mikael and C.L. Max, "Pressure sensors based on suspended graphene membranes", *Solid-State Electronics*, vol. 88, pp. 89-94, June. 2013.

[9] O.K. Kwon, J.H. Lee, K.S. Kim and J.W. Kang, "Developing ultrasensitive pressure sensor based on graphene nanoribbon: molecular dynamics simulation", *Physica E*, vol. 47, pp. 6-11, Oct. 2013.

[10] J.S. Bunch, A.M. van der Zande, S.S. Verbridge, I.W. Frank, D.M. Tanenbaum, J.M. Parpia, H.G. Craighead and P.L. McEuen, "Electromechanical resonators from graphene", *Science*, vol. 315, pp. 490-493, Jan. 2007.

[11] E. Paek and G.S. Hwang, "A computational analysis of graphene adhesion on amorphous silica", *J. Appl. Phys.*, vol. 113, pp. 164901, Apr. 2013.

[12] Y. He, W.F. Chen, W.B. Yu, G. Ouyang and G.W. Yang, "Anomalous interface adhesion of graphene membranes", *Scientific Report*, vol. 3, pp. 2660, Sep. 2013.

[13] Z. Zong, C.L. Chen, M.R. Dokmeci, K.-tak Wan, "Direct measurement of graphene on silicon surface by intercalation of nanoparticles", *J. Appl. Phys.*, vol. 107, pp. 026104, Jan. 2010.

[14] J.S. Bunch and M.L. Dunn, "Adhesion mechanics of graphene membranes", *Solid State Communications*, vol. 152, pp. 1359-1364, Apr. 2012.

[15] S.P. Koenig, N.G. Boddeti, M.L. Dunn and J.S. Bunch, "Ultra-strong adhesion of graphene membranes", *J. Nat. Nanotechnol.*, vol. 6, pp. 543-546, Aug. 2011.

[16] N.G. Boddeti, S.P. Koenig, R. Long, J.L. Xiao, J.S. Bunch and M.L. Dunn, "Mechanics of adhered pressurized graphene blisters", *Journal of Applied Mechanics*, vol. 80, pp. 040909, May. 2013.

[17] T. Yoon, W.C. Shin, T.Y. Kim, J.H. Mun, T.S. Kim and B.J. Cho, "Direct measurement of adhesion energy of monolayer graphene as-grown on copper and its application to renewable transfer process", *Nano Letters*, vol. 12, pp. 1448-1452, Feb. 2012.

[18] S. Das, D. Lahiri, D.Y. Lee, A. Agarwal and W.B. Choi, "Measurements of the adhesion energy of graphene to metallic substrates", *Carbon*, vol. 59, pp. 121-129, Mar. 2013.
[19] T. Jiang and Y. Zhu, "Measuring graphene adhesion using atomic force microscopy with a microsphere tip", *Nanoscale*, vol. 7, pp. 10760, May. 2015.
[20] C. Li, J. Xiao, T.T. Guo, S.C. Fan and W. Jin, "Interference characteristics in a Fabry-Perot cavity with graphene membrane for optical fiber pressure sensors" *Microsystem Technologies*, vol. 21, no. 11, pp. 2297-2306, Nov. 2015.
[21] J.J. Vlassak and W.D. Nix, "A new bulge test technique for the determination of Young's modulus and Poisson's ratio of thin films", *J. Mater. Res.* vol. 7, no. 12, pp. 3242-3249, Aug. 1992.
[22] H. Sun, X.L. Zhang, L.T. Yuan, L.B. Zhou, X.G. Qiao and M.L. Hu, "An optical fiber Fabry-Perot interferometer sensor for simultaneous measurement of relative humidity and temperature", *IEEE Sensors Journal*, vol. 15, no. 5, pp. 2891-2897, May. 2015.
[23] C. Ma, B. Dong, J.M. Gong and A.B. Wang, "Decoding the spectra of low-finesse extrinsic optical fiber Fabry-Perot interferometers," *Opt. Express*, vol. 19, no. 24, pp. 23727-23742, Nov. 2011.
[24] B. Yu, D.W. Kim, J.D. Deng, H. Xiao and A.B. Wang, "Fiber Fabry-Perot sensors for detection of partial discharges in power transformers," *Appl. Opt.*, vol. 42, no. 16, pp. 3241-3250, July. 2003.
[25] C. Li, X.Y. Gao, T.T. Guo, J. Xiao, S.C. Fan and W. Jin, "Analyzing the applicability of miniature ultra-high sensitivity Fabry-Perot acoustic sensor using a nanothick graphene diaphragm", *Meas. Sci. Technol.* vol. 26, no. 8, pp. 085101, Nov. 2015.
[26] D.X. Wang, S.C. Fan and W. Jin, "Graphene diaphragm analysis for pressure or acoustic sensor applications", *Microsyst. Technol.*, vol. 21, no. 1, pp.117-122, Jan. 2015.
[27] Ge ́minard J.C., Bernal R. and Melo F. "Wrinkle formations in axisymmetrically stretched membranes", *Eur. Phys. J. E*, vol. 15, pp. 117-126, Nov. 2004.
[28] F.J. Nelson, V.K. Kamineni, T. Zhang, E.S. Comfort, J.U. Lee and A.C. Diebold, "Optical properties of large-area polycrystalline chemical vapor deposited graphene by spectroscopic ellipsometry," *Applied Physics Letters*, vol. 97, no. 25, pp. 253110, Dec. 2010.
[29] H.S. Skulason, P.E. Gaskell and T. Szkopek, "Optical reflection and transmission properties of exfoliated graphite from a graphene monlolayer to several hundred graphene layers," *Nanotechnology*, vol. 21, pp. 295709, July. 2010.
[30] C. Li, Q.W. Liu, T.T. Guo, J. Xiao, S.C. Fan and W. Jin, "An ultra-high sensitivity Fabry-Perot acoustic pressure sensor using a multilayer suspended graphene diaphragm". in *Proc. IEEE Sensors*,2015, pp. 567-570.
[31] X.Y. Zhao, D. Ceresoli and D. Vanderbilt, "Structural, electronic, and dielectric properties of amorphous ZrO_2 from *ab initio* molecular dynamics", Physical Review B, vol. 71, pp, 085107, Feb. 2005.
[32] Campbell J.D. "On the theory of initially tensioned circular membranes subjected to uniform pressure", *J. Mech. Appl. Math.*, vol. 9, no. 1, pp.84-93, Jan. 1956.
[33] W.H. Wang, S.D. Li and L.L. Wen, "Ultra-low sensitivity to temperature low-cost optical fiber Fabry-Perot micro pressure sensor with a chitosan diaphragm", *Optics Communications*, vol. 309, pp. 302-306, Aug. 2013.
[34] G. Hill, R. Melamud, F.E. Declercq, A.A. Davenport, I.H. Chan, P. Hartwell and B.L. Pruitt, "SU-8 MEMS Fabry-Perot pressure sensor", *Sensors and Actuators A: Physical*, vol. 138, no. 1, pp. 52-62, July. 2007.
[35] W. Wang, N. Wu, Y. Tian, C. Niezrecki and X.W. Wang, "Miniature all-silica optical fiber pressure sensor with an ultrathin uniform diaphragm", *Optics Express*, vol. 18, no. 9, pp. 9006-9014, April. 2010.
[36] F. Xu, D.X. Ren, X.L. Shi, C. Li, W.W. Lu, L. Lu, L. Lu and B.L. Yu, "High-sensitivity Fabry–Perot interferometric pressure sensor based on a nanothick silver diaphragm", *Optics Letters*, vol. 37, no. 2, pp. 133-135, January. 2012.

Cheng Li received the B.S. and M.S. degrees from Hebei University of Technology, Tianjin, China, in 1999 and 2002, respectively. He received the Ph.D. degree in instrument science and technology from Tsinghua University, Beijing, China, in 2007 and afterwards was employed as a Postdoctoral Research Fellow at the same University till 2009. Then he joined the Department of Instrumentation Science and Opto-electronics Engineering, Beihang University, where he currently serves as an associate professor. During the year in 2011, he was a short-term visiting scholar with the School of Electrical and Electronic Engineering at Nanyang Technological University, Singapore.

His research interests are graphene-based optical fiber sensors, and acoustic signal processing and transmission technology. He is a committee member of Sensor Branch of China Instrument and Control Society and a deputy secretary general of Beijing Minimally Invasive Medical Society.

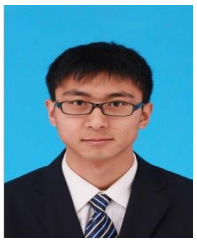

Xiangyang Gao received the B.S degree in mechanical engineering from Tianjin University, Tianjin, China in 2010. He is currently pursuing the M.S. degree at the Department of Instrumentation Science and Opto-electronics Engineering, Beihang University, Beijing, China.

His research interests are optical fiber sensors and adhesion behaviors at membrane-substrate interface.

Shangchun Fan received the M.S. and Ph.D degrees in instrumentation science and technology from Beihang University, Beijing, China, in 1986 and 1990, respectively. He is currently a Professor with the Department of Instrumentation Science and Opto-electronics Engineering, Beihang University, China.

His research interests include sensor fundamentals and applications, intelligent measurement techniques and systems. He is a senior member of IEEE, an executive committee of China Instrument and Control Society, and a vice president of Sensor branch of China Instrument and Control Society.

Dongxue Wang received the B.S. degree in electrical engineering from Shandong Jianzhu University, Shandon, China, in 2005 and the M.S. degree in control theory and control engineering from Jinan University, Shandong, China, in 2008. He received the Ph.D. degree in instrument science and technology from Beihang University, Beijing, China, in 2015. Currently, he is a lecturer with Jinan University, China.

His research interests include high precision pressure sensor and weak electrical signal detection.

Wei Jin received the B.S. and M.S. degrees from Beihang University, Beijing, China, in 1984 and 1987, respectively. He received the Ph.D. degree in 1991 in fiber optics from University of Strathclyde and afterwards was employed as a Postdoctoral Research Fellow at the same University till the end of 1995. He joined the Department

of Electrical Engineering of the Hong Kong Polytechnic University as an assistant Professor in 1996 and was promoted to an associate professor in 1998 and a professor in 2003.

His research interests are photonic crystal fibers and devices, optical fiber sensors, fiber lasers and amplifiers, optical gas detectors, condition monitoring of electrical power transformers, and civil and mechanical structures.

He is a senior member of IEEE, a member of SPIE and OSA, and a vice Chairman of the Fiber and Integrated Society of China. He has served as a Technical Program Committee member/session chair of over 20 international and national conferences.